The Influence of the Equilibrium Melting Temperature on the Supermolecular Morphology of Several Polymers

C. J. MURPHY,[1,*] J. J. FAY,[2] E. A. M. VAIL,[2] and L. H. SPERLING[3]

[1]Department of Chemistry, East Stroudsburg University, East Stroudsburg, Pennsylvania 18301; [2]Department of Chemistry and [3]Departments of Chemical Engineering and Materials Science and Engineering, Materials Research Center, Center for Polymer Science and Engineering, Whitaker Laboratory #5, Lehigh University, Bethlehem, Pennsylvania 18015

SYNOPSIS

At a constant isothermal crystallization temperature (T_c), the crystalline morphologies of several polymers have been found to be a function of the melt-liquid temperature (T_1). At a constant T_c below a critical crystallization temperature T_c^* [about 0.9 T_m^* (K)], a transition from a nonspherulitic to a spherulitic morphology occurs when the melt liquid is heated above a melt-liquid transition temperature, (T_{lt}) [approximately 1.03 T_m (K)], where T_m is the observed melting temperature of the sample. The melt-liquid transition temperature, T_{lt}, which experimentally affects the visible morphology of a semicrystalline polymer, is apparently indistinguishable from the thermodynamic melting temperature, T_m^*, determined by the Hoffman–Weeks procedure. The X-ray powder diffraction patterns of spherulitic and nonspherulitic morphologies were identical, independent of the heating–cooling cycle. This suggests that the transition that occurs at T_{lt} does not affect the arrangement of polymer molecules in the crystallite, but only the manner in which the crystallites are arranged in the supermolecular morphology. The evidence suggests, at least for the polymers studied, that a residual order exists in the melt until the T_m^* or T_{lt} of the particular polymer is reached. © 1993 John Wiley & Sons, Inc.

INTRODUCTION

The elementary crystal structure of a homopolymer crystallized from the melt is the lamellar crystallite. Under appropriate conditions, crystallites can be organized into higher levels of crystalline morphology or supermolecular structure, such as hedrites, axialites, or spherulites.[1] The morphology of a polymer crystallized from the melt in any given experiment depends on a number of factors, including crystallization temperature, polymer molecular weight and polydispersity index, the cooling rate, and polymer film thickness. These relationships have been correlated into morphology maps by Mandelkern and co-workers.[2,3]

The relationships between the crystal structure, gross morphology, and properties of polymers have been extensively reviewed for polymers, in general, by Mandelkern[4] and for polyethers, in particular, by Fatou.[5] The crystallization behavior of several polyoxetanes, first synthesized by Farthing in 1955,[6,7] have been reported in recent years with differences correlated to the nature of the pendant groups on the polyoxetane backbone chain.[8–13] In addition, the effect of melt history on semicrystalline polymers has been reviewed by Rault.[14]

This is the seventh paper[15–20] in a study of homopolymers and block copolymers based on poly[3,3-bis(ethoxymethyl)oxetane] (polyBEMO) and related polyethers.[21] In one of these,[17] evidence was presented that a relationship exists between the equilibrium melting temperature (T_m^*), determined by the Hoffman–Weeks procedure, and the gross morphologies observed microscopically. In particular, polymer melts heated to a melt-liquid temperature, T_l, above T_m^* formed spherulites on crystallization when cooled below some threshold temperature. On the other hand, polymer melts heated to

* To whom correspondence should be addressed.

Journal of Applied Polymer Science, Vol. 48, 1321–1329 (1993)
 CCC 0021-8995/93/081321-09

a melt-liquid temperature below T_m^*, then cooled to the same crystallization temperature, formed hedritic or fine-grained supermolecular morphologies, which could not be resolved by light microscopy. The results were independent of the time the melt was held at a particular temperature and of the particular morphology that was melted. In another paper,[20] the observed multiple endotherm melting behavior of polyBEMO was observed and related to melt-liquid temperature history, molecular weight, and morphology.

In this paper, values of T_m^* for several additional polymers will be presented. Evidence will also be presented that extends the relationship among T_l, T_m^*, and the observed morphology to several additional semicrystalline polymers. In addition, the apparent relationship between the experimental melting temperature, T_m, the equilibrium melting temperature, T_m^*, and an apparent liquid–liquid transition temperature, T_{lt}, at about 1.03 T_m (K) will be examined.

EXPERIMENTAL

Materials

The polymers used in this study were poly[3,3-bis(methoxymethyl)oxetane] (polyBMMO), poly[3,3-bis(ethoxymethyl)oxetane] (polyBEMO), poly[3,3-bis(chloromethyl)oxetane] (polyBCMO), poly[3,3-bis(azidomethyl)oxetane] (polyBAMO), poly(ethylene oxide) (PEO), polypropylene (PP); poly(ethylene glycol) (PEG), and nylon 66. The syntheses of polyBEMO, polyBMMO, and polyBAMO have been described previously.[15–18] Samples of the remaining polymers were obtained from the following suppliers and used as received: PEO, M_w = 100,000 g/mol (Aldrich Chemical Co.); polyBCMO (BDH); PP, M_w = 260,000 g/mol (Scientific Polymer Products); nylon 66 (Scientific Polymer Products); and PEG, M_w = 12,600 g/mol (Polymer Laboratories and Polysciences). The structures, molecular weights, and polydispersity indexes, where available, of the polymers are given in Table I.

Instrumentation

Optical microscopy studies of morphologies were made using a Zeiss 20-T microscope equipped with reflecting and transmitting polarized-light Nomarski optics, a Zeiss M-35 automatic exposure camera, and a LinKam TH600 microprocessor controlled hotstage, calibrated with 1,3-diphenylbenzene (T_m 59–61°C), *m*-toluic acid (T_m 108–110°C), and DL-mandelic acid (T_m 120–122°C) (Aldrich Chemical Co. melting point standards).

X-ray powder diffraction studies were performed using a Phillips APD 3720 automated X-ray powder diffractometer with a copper target and a Phillips XRG X-ray generating unit. A nickel filter was used to isolate the CuKα line (λ = 1.542 A). A scan rate of 1°/min with 0.02° increments was used.

Molecular weights were estimated, for polymers soluble in tetrahydrofuran, using a Waters gel permeation chromatograph (GPC) calibrated with polystyrene standards using tetrahydrofuran as solvent or were as given by the supplier.

Procedures and Definitions

The several procedures used and procedure-related definitions are as follows:

1. Melting temperature: The experimental melting temperature (T_m) was taken as the temperature at which the last visible trace of crystallinity disappeared and the sample became a clear isotropic liquid, as observed between crossed polarizers. At the same heating rates, T_m determined by this method correlates closely with the peak temperature of the melting endotherm as determined by DSC and is about 10°C lower than the temperature at which the DSC peak returns to the base line.[19]
2. Crystallization temperature: The crystallization temperature (T_c) was the temperature at which isothermal crystallization occurred.
3. Melt-liquid temperature: The melt-liquid temperature (T_l) was the temperature above T_m to which the polymer melt was heated. The liquid was held at T_l for 30–60 s before the cooling cycle was initiated. Variation of the time the polymers were held at T_l from 5 s to 6 h appeared to have no effect on the morphology observed.
4. Equilibrium melting temperature: The equilibrium melting temperature (T_m^*), as determined by the Hoffman–Weeks procedure, is defined as the thermodynamic condition where $T_m = T_c$; that is, the polymer crystal is perfect and in thermodynamic equilibrium with the melt.[22–25] Operationally, T_m^* was determined experimentally from the intersection of the least-squares plot of T_m vs. T_c with the line representing $T_m = T_c$.[24,25]

Table I Structures and M_w of Polymers

Polymers	Abbreviation	Structure	M_w (g/mol)	Polydispersity Index (M_w/M_n)
Poly[3,3-bis(methoxymethyl) oxetane]	PolyBMMO	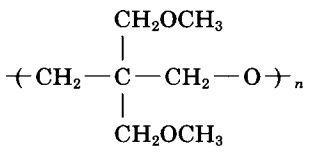	40,000	—
Poly[3,3-bis(ethoxymethyl) oxetane]	PolyBEMO	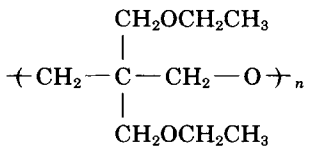	74,000	2.5
Poly[3,3-bis(azidomethyl) oxetane]	PolyBAMO	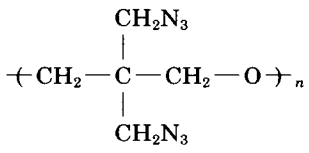	51,000	2.0
Poly[3,3-bis(chloromethyl) oxetane]	PolyBCMO	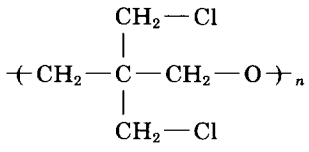	—	—
Poly(ethylene oxide)	PEO	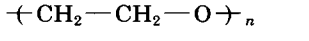	100,000	—
Polypropylene	PP	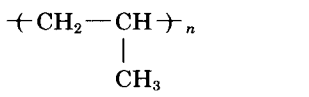	260,000	—
Poly(ethylene glycol)[a]	PEG	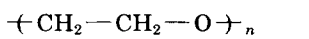	12,600	1.2
Poly(hexamethylene adipamide)	Nylon 66	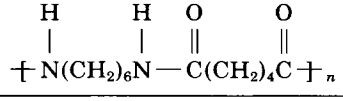	27,500	2.2

[a] Same as PEO, but with —OH groups on both ends.

5. Melt-liquid transition temperature: The melt-liquid temperature at which a transition from a nonspherulitic to a spherulitic morphology was observed on isothermal crystallization at a given T_c is designated as T_{lt}.
6. Thermal evaluation of samples: Typically, thin-film samples between coverglasses were evaluated by raising the temperature at a rate of 10°C/min to T_m, which was recorded, then at the same rate to T_l, at which temperature the sample was held for 30–60 s. The temperature was then reduced at a rate of 30°C/min to T_c, which was maintained until isothermal crystallization was complete. Depending on the extent of undercooling, crystallization typically began at least 30 s after T_c was reached. The cooling rate had no effect on the observed morphology. The morphology was noted and the cycle was repeated from five to ten times.

Samples for X-ray powder diffraction studies were prepared by melting the polymer directly on a glass sample plate, heating to a T_l, either above or below T_m^*, then cooling to T_c and allowing the sample to crystallize isothermally. The morphology of each sample was observed by visible light microscopy before the X-ray powder pattern was determined.

RESULTS

The values of T_m^* for the various polymers, determined by the Hoffman–Weeks procedure, are given in Table II. The values of T_m^* for polyBEMO and polyBAMO have been reported previously,[17] whereas the values for PEO and PP are within the range reported in the literature.[5]

The gross morphologies of the various polymers as a function of T_c and T_l were determined by polarized light microscopy. Photographs of the observed morphologies of PEO, polyBEMO, and polyBAMO were previously published.[17] Microphotographs of the observed morphologies of the additional polymers are shown in Figure 1. For each of the polymers when a constant T_c is chosen, the observed morphology is dependent only on the T_l to which the polymer melt is heated. In general, when a polymer melt is heated to a T_l below the T_m^* of that specific polymer, a nonspherulitic morphology, such as hedritic, rodlike, or fine-grained is observed. On the other hand, when the polymer melt is heated to a T_l above T_m^*, spherulitic morphologies are observed. The morphology observed in any given instance, at constant T_c, was dependent only on the T_l attained, not on the morphology that was observed before melting. For example, if a spherulitic sample of polyBEMO was melted and the melt liquid was heated to a T_l below the T_m^* of polyBEMO, a nonspherulitic morphology was obtained on crystallization. If the sample was then melted and the melt liquid was heated to a T_l above the T_m^* of polyBEMO, cooled to the same T_c as before, and crystallized, a spherulitic morphology was regained.

The morphologies previously published[17] and those depicted in Figure 1 are quantified in Tables III and IV. In Table III, when the T_l was increased at constant T_c for the various polymers, the morphologies were observed to change from fine-grained or hedritic to spherulitic over a transition range of from 1 to 10°C in T_l. The midpoint of the temperature range at which this transition in morphology was observed was designated T_{lt}.

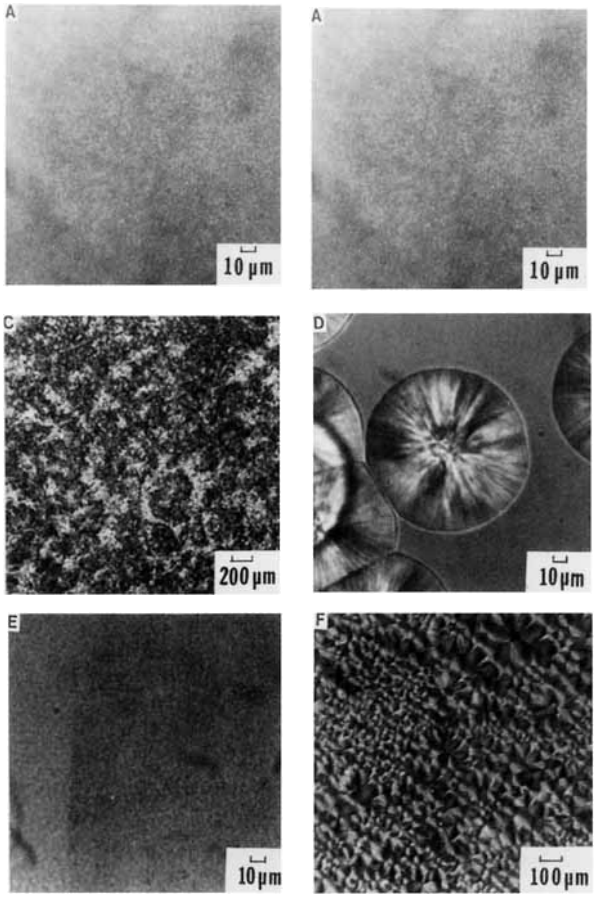

Figure 1 Optical micrographs of morphologies obtained by heating samples to T_l and crystallizing at T_c: (A) polyBCMO, T_l = 185°C, T_c = 155°C; (B) polyBCMO, T_l = 200°C, T_c = 155°C; (C) PP, T_l = 170°C, T_c = 120°C; (D) PP, T_l = 228°C, T_c = 125°C; (E) polyBMMO, T_l = 95°C, T_c = 60°C; (F) polyBMMO, T_l = 120°C, T_c = 60°C.

Table II Thermodynamic Melting Temperatures

Polymer	T_m^* (K)
PolyBEMO	365
PolyBAMO	375
PolyBMMO	366
PolyBCMO	461
PEO	342
PP	478

The inverse experiment was also performed and the results are shown in Table IV. At a constant melt-liquid temperature slightly higher than the T_{lt} observed above, the morphology observed for a particular polymer became more obviously spherulitic as the isothermal crystallization temperature, T_c, was lowered. The T_c above which spherulites are not observed in this experiment is designated T_c^*. If the melt-liquid temperature is held below the T_{lt} for a particular polymer, spherulitic morphologies were never observed, regardless of the T_c.

As shown in Figure 2, the X-ray powder patterns for spherulitic (T_l = 120°C, T_c = 50°C) and nonspherulitic (T_l = 90°C, T_c = 50°C) polyBEMO were

Table III Variation of Morphology with T_l at Constant T_c

T_l (Ref. 17) (K)	T_l/T_m	Morphology (Ref. 17)
PolyBEMO: T_c = 323 K, T_m = 355 K		
393	1.107	Spherulitic
383	1.079	Spherulitic
373	1.051	Spherulitic
368	1.037	Mixed spherulitic and hedritic
363	1.022	Hedritic
358	1.008	Hedritic
T_l (K)	T_l/T_m	Morphology
PolyBMMO: T_c = 323 K, T_m = 361.8 K		
378	1.045	Spherulitic
373	1.031	Mixed
368	1.017	Nonspherulitic
T_l (Ref. 17) K	T_l/T_m	Morphology (Ref. 17)
PolyBAMO: T_c = 323 K, T_m = 362.7 K		
393	1.084	Spherulitic
383	1.056	Spherulitic or hedritic
378	1.042	Mixed hedritic and fine-grained
373	1.028	Mixed hedritic and fine-grained
368	1.015	Fine-grained
PEO: T_c = 323 K, T_m = 334.8 K		
343	1.024	Spherulitic
341	1.019	Spherulitic
340	1.016	Spherulitic
338	1.010	Spherulitic
336	1.004	Mixed spherulitic and hedritic
335	1.001	Hedritic
T_l (K)	T_l/T_m	Morphology
PolyBCMO: T_c = 423 K, T_m = 454.2 K		
483	1.063	Spherulitic
473	1.041	Spherulitic
463	1.019	Nonspherulitic
458	1.008	Nonspherulitic
PP: T_c = 403 K, T_m = 441.6 K		
483	1.094	Spherulitic
473	1.071	Spherulitic
463	1.048	Mixed
453	1.026	Fine-grained
443	1.003	Fine-grained
PEG: 12.6 K, T_c = 323 K, T_m = 337 K		
340	1.009	Spherulitic
339	1.006	Spherulitic
338	1.003	Mixed
337	1.000	Rods
Nylon 66; T_c = 508 K, T_m = 535 K		
553	1.034	Starlike
543	1.015	Fine-grained
538	1.006	Fine-grained

found to be identical, as were the X-ray powder patterns of spherulitic (T_l = 120°C, T_c = 50°C) and nonspherulitic (T_l = 90°C, T_c = 50°C) polyBAMO.

DISCUSSION

Relationship between T_m^* and T_{lt}

Evidence has been presented in previous papers in this series that a relationship exists between the melt-liquid temperature, T_l, the equilibrium melting temperature determined by the Hoffman–Weeks procedure, T_m^*, and the observed supermolecular morphologies of homopolymers of polyBEMO, polyBAMO, and PEO[17] and block copolymers of polyBEMO and polyBAMO.[19] This relationship has now been extended to additional polymers and new implications of the phenomena have become apparent.

The data in Table III show that for the polymers studied the observed supermolecular morphology is a function of T_l at constant T_c. At constant T_c, the supermolecular morphology depends only on T_l, not on the previous morphology or on the time the polymer melt liquid was held at T_l. In general, a tran-

Table IV Variation of Gross Morphology with T_c at Constant T_l

T_c (K)	T_m (K)	Morphology
	PolyBEMO: T_l = 383.1 K	
333.1	357.3	Hedritic
328.1	355.3	Irregular spherulitic
323.1	354.7	Spherulitic
318.1	353.2	Spherulitic
313.1	352.4	Spherulitic
	PolyBAMO: T_l = 383.1 K	
338.1	366.3	Hedritic
333.1	363.3	Irregular spherulitic
328.1	362.9	Spherulitic
323.1	362.4	Spherulitic
	PolyBMMO: T_l = 393.1 K	
333.1	361.6	Fine-grained
328.1	362.6	Spherulitic
323.1	361.8	Spherulitic
318.1	361.6	Spherulitic

sition from a nonspherulitic to a spherulitic morphology will occur over some range of T_l. The midpoint of this range may be designated as T_{lt}, which is approximately equal to the T_m^* of a particular polymer, as seen below.

In Figure 3, the T_{lt} determined from the data in Table III is compared with the values of T_m^* for several polymers. It is apparent that a high correlation, well within experimental error, exists between T_m^* and T_{lt}. It should be recognized that the methods of determining the two values are markedly different. T_m^* is an extrapolated temperature that represents the thermodynamic equilibrium of a perfect crystal in the melt liquid. Comparatively, T_{lt} is an experimentally observed transition temperature between different morphologies. Usually, the transition in the observed morphology occurs over a few to a several degree range of T_l, at constant T_c. The morphology of some polymers are very sensitive to T_l, with changes of less than 1°C resulting in a change in the observed morphology. Qualitatively, the phenomenon appears to be shown more clearly by lower molecular weight samples than for higher molecular weight samples of the same polymer. Additionally, in samples of similar molecular weight ($M_n \sim 1.1 \times 10^4$ g/mol), a polymer of lower melt viscosity, such as polyBEMO (η = 8 P), showed the effect more clearly than did a polymer of higher melt viscosity, such as polyBAMO (η = 62.5 P).

As shown in Figure 2, the X-ray powder patterns of spherulitic and nonspherulitic polyBEMO and polyBAMO samples were unchanged by the heating

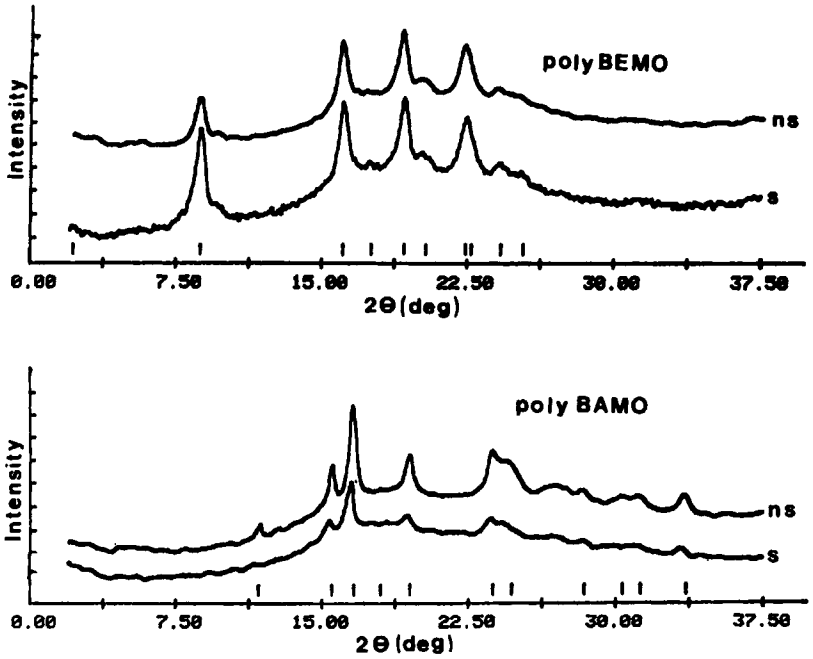

Figure 2 X-ray powder diffraction patterns of polyBEMO and polyBAMO.

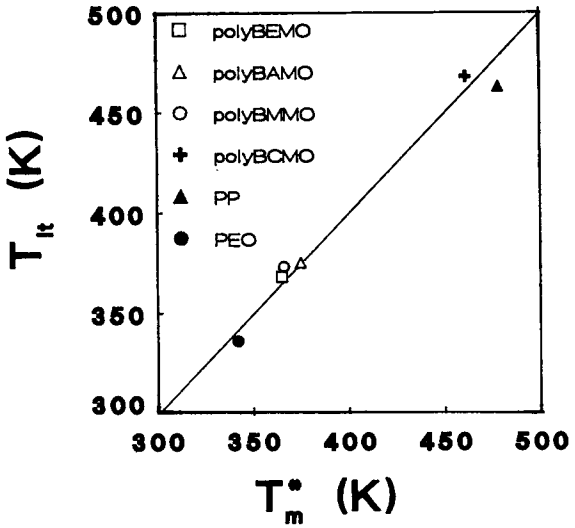

Figure 3 Comparison of T_{lt} and T_m^* for several polymers.

and cooling cycle variations; that is, the crystal structure of a nonspherulitic sample of a polymer heated to a T_l below T_{lt} was the same as a spherulitic sample heated to a T_l above T_{lt}. This implies that the transition that occurs at T_{lt} affects only the manner in which the polymers crystallites are arranged in the supermolecular morphology, not the arrangement of the polymer molecules in the crystallite.

From the data in Table III, it can be seen that the transition from an observed nonspherulitic to an observed spherulitic morphology on crystallization occurs at a ratio of T_l/T_m (K) of from about 1.006 for PEG to about 1.05 for polyBAMO, with a median of approximately 1.03. Thus, a transition between observed morphologies occurs at $\sim 1.03\ T_m$ (K), which may be designated as T_{lt}, the melt-liquid transition temperature.

For each of the polymers studied, as shown in Figure 3, the value of the melt-liquid transition temperature between semicrystalline morphologies, T_{lt}, and the thermodynamic equilibrium melting temperature, T_m^*, are equal within experimental error.

Several explanations of the observations are possible. In one, the existence of subcritical nuclei can be assumed to be present in the melt liquid between T_m and T_m^*. Although this assumption cannot be rigorously ruled out, the results of the present study suggest otherwise. When samples are heated to a T_l above T_m^*, then held in the melt at temperatures between T_m and T_m^* for some time before isothermal crystallization, spherulitic morphologies are obtained. If subcritical nuclei were present, a fine-grained morphology would probably result.

Another possible explanation is if one starts with a spherulitic sample of a polymer and heats it to T_m, a transition occurs to an apparently isotropic liquid. This liquid, however, retains considerable local order related to the arrangement of the polymer molecules in the crystallite. At T_{lt}, which is $\sim 1.03\ T_m$ (K), a transition to a less ordered liquid state occurs. This quantity T_{lt} can be considered equivalent to T_m^*, which is the extrapolated T_m of an infinitely large perfect crystal, that is, the highest temperature at which crystalline order can exist for a given polymer. Upon cooling to T_c from a melt-liquid temperature above T_m^*, crystallization begins at isolated, heterogeneous nucleation sites and the polymer crystallites have sufficient time to organize themselves into a spherulitic morphology. On the other hand, when the polymer melt liquid is heated only to a temperature below T_{lt}, the local order in the crystallite is not disrupted. Thus, when the sample is cooled to an isothermal T_c, the residual local order induces homogeneous crystallization simultaneously throughout the sample, resulting in the observed sudden appearance of a nonspherulitic morphology.

The difference between spherulitic and nonspherulitic morphologies can be related to the arrangements of polymer crystallites in the supermolecular structure. It is apparently not related to the arrangement of the polymer molecule in the crystallite as the X-ray powder patterns are identical for spherulitic and nonspherulitic samples of a given polymer crystallized at the same isothermal T_c. Crystal structure is a known function of T_c and solid-state transitions between crystal structures are well known. The formation of a spherulitic morphology in the studied polymers, in addition, appears to be related to having T_l exceed some critical temperature, which may be designated alternatively as T_{lt}, the transition temperature from a liquid with local order to one with much less order or as T_m^*, the thermodynamic melting temperature.

The melts between T_m and T_m^* are clear, and, hence, any physically ordered regions must be small. The forces holding the ordered regions together may also be very weak. In the present work, all materials were quiescent, held between microscope coverglasses. In a dynamic viscosity experiment, or even a steady shear experiment, the possibility of disrupting the residual local order would need to be considered. This may be related to the difficulty in observing the phenomenon in a dynamic experiment.

Relationship between T_c^* and Hoffman's Regimes

As noted in Table IV, at a constant T_l above T_m^*, the transition from a nonspherulitic morphology to a spherulitic morphology occurs as the isothermal crystallization temperature decreases. The T_c at which this transition occurs is designated T_c^*.

Considerable research has been carried out in the area of polymer crystallization kinetics, including that by Hoffman et al.[23] They developed a quantitative model that defines three regimes of crystallization kinetics for polyethylene melts.[24] Briefly, the three regimes differ in the rate of crystallization as well as in the manner in which the polymer chains are incorporated onto the growing lamella surface. During isothermal crystallization of polyethylene within the temperature region of regime I, which occurs at small supercooling, axialites are formed. Comparatively, at larger supercoolings in the region of regime II, spherulitic morphologies are observed. Finally, regime III kinetics are obtained in instances where there are very large supercoolings. Thus, it is likely that the transition, T_c^*, observed in the present lies at the boundary between regimes I and II crystallization kinetics.

The growth rates obtained for various samples show a discontinuity between regimes I and II, which coincides with the observed change in morphology.[23] The ratio of the crystallization temperature at the discontinuity to the estimated equilibrium melting temperature (T_c^*/T_m^*) of polyethylene is 0.93. This value is approximately the same as the values of T_c^*/T_m^* calculated for polyBEMO, polyBAMO, and polyBMMO as shown in Table V. Furthermore, Hoffman et al.[25] also noted that for very low and very high molecular weight polyethylene samples the transition from regime I to regime II kinetics is broadened, which corroborates some of the experimental observations made in the present study.

Thermodynamic considerations apparently come to the fore in the melt state in the vicinity of the melt-liquid transition temperature, T_{lt}, or the equilibrium melting temperature, T_m^*. Crystallization kinetics, however, may also contribute to the determination of crystalline morphology, especially when the melt-liquid temperature exceeds T_{lt} or T_m^*.

The necessary conditions for spherulite formation are that the polymer must first be heated above T_m^*, then cooled below T_c^*. Maintaining conditions between these factors results in fine-structured crystallization. There is an essentially constant ratio of 0.89–0.93 of T_c^* to T_m^*, for the polymers for which data is available, as shown in Table V.

Table V Critical Crystallization Temperatures

Polymer	T_c^* (From Table IV)	T_m^* (From Table II)	T_c^*/T_m^*
BEMO	328	365	0.90
BAMO	333	375	0.89
BMMO	333	366	0.91
PE[23]	400	431	0.93

CONCLUSIONS

The supermolecular morphology observed at a given T_c was found to vary with T_l for the polymers studied. If T_l is held below the transition temperature T_{lt}, which is approximately 1.03 T_m (K) or T_m^*, nonspherulitic morphologies are observed. However, if T_l is raised above T_{lt}, spherulitic morphologies are obtained on isothermal crystallization if the T_c is below a critical crystallization temperature T_c^*, which is about 0.89–0.93 T_m^*. T_{lt} appears to be related to a transition from a liquid state that retains the local order of the crystallite to a liquid state with little or no local order. The identity of the X-ray powder patterns for spherulitic and nonspherulitic samples of the same polymer suggests that the transition does not change the way polymer molecules are arranged in the crystallite, but does affect the manner in which the crystallites are arranged in the supermolecular morphology. These observations suggest that the mechanical properties of polymers, which are known to improve as spherulite size is decreased, can be further improved by suppressing spherulite formation completely by keeping the processing temperature of a semicrystalline polymer below T_{lt} or about 1.03 T_m (K) or by crystallizing at temperatures greater than T_c^*, which is about 0.90 T_m^* (K).

The authors wish to thank the Office of Naval Research for support through Contract No. N00014-82-K-0050 and Mr. Gerry Manser of Aerojet Strategic Propulsion Co., Sacramento, CA, for samples of the polyethers.

REFERENCES

1. L. Mandelkern, *Discuss. Faraday Soc.*, **68,** 310 (1980).
2. I. G. Voight-Marten and L. Mandelkern, *J. Polym. Sci. Polym. Phys. Ed.*, **19,** 1769 (1981).
3. R. C. Allen and L. Mandelkern, *J. Polym. Sci. Polym. Phys. Ed.*, **20,** 1465 (1982).

4. L. Mandelkern, in *Physical Properties of Polymers,* J. E. Mark, A. Eisenberg, W. W. Graessley, L. Mandelkern, and J. L. Koenig, Eds., American Chemical Society, Washington, DC, 1984.
5. J. G. Fatou, *Makromol. Chem. Suppl.,* **7,** 131 (1984).
6. A. C. Farthing, *J. Chem. Soc.,* 3638 (1955).
7. A. C. Farthing, *J. Appl. Chem.,* **8,** 186 (1958).
8. E. Perez, M. A. Gomez, A. Bello, and J. G. Fatou, *Coll. Polym. Sci.,* **261,** 571 (1983).
9. M. A. Gomez, E. Perez, A. Bello, and J. G. Fatou, *Polym. Commun.,* **27,** 166 (1986).
10. M. A. Gomez, J. G. Fatou, and A. Bello, *Eur. Polym. J.,* **22,** 661 (1982).
11. E. Perez, A. Bello, and J. G. Fatou, *Makromol. Chem.,* **190,** 613 (1987).
12. J. Brandup and E. H. Immergut, *Polymer Handbook,* 3rd ed., Wiley-Interscience, New York, 1989, p. VI–75.
13. D. J. H. Sandiford, *J. Appl. Chem.,* **8,** 188 (1958).
14. J. Rault, *CRC Crit. Rev. Solid State Mat. Sci.,* **13**(1), 57 (1986).
15. R. B. Jones, C. J. Murphy, L. H. Sperling, M. Farber, S. P. Harris, and G. E. Manser, *J. Appl. Polym. Sci.,* **30,** 95 (1985).
16. K. E. Hardenstine, G. V. S. Henderson, L. H. Sperling, C. J. Murphy, and G. E. Manser, *J. Polym. Sci. Polym. Phys. Ed.,* **23,** 1597 (1985).
17. C. J. Murphy, G. V. S. Henderson, E. A. Murphy, and L. H. Sperling, *Polym. Sci. Eng.,* **27,** 781 (1987).
18. K. E. Hardenstine, C. J. Murphy, R. B. Jones, L. H. Sperling, and G. E. Manser, *J. Appl. Polym. Sci.,* **30,** 2051 (1985).
19. E. A. Murphy, T. Ntozakhe, C. J. Murphy, J. J. Fay, and L. H. Sperling, *J. Appl. Polym. Sci.,* **37,** 267 (1989).
20. J. J. Fay, C. J. Murphy, and L. H. Sperling, *J. Appl. Polym. Sci.,* **40,** 1379 (1990).
21. G. E. Manser (Thiokol), U.S. Pat. 4,393,199 (1983).
22. J. D. Hoffman and J. J. Weeks, *J. Res. Natl. Bur. Stand.,* **66A,** 13 (1962).
23. J. D. Hoffman, G. T. Davis, and J. I. Lauritzen, Jr., in *Treatise on Solid State Chemistry,* Vol. 3, *Crystalline and Noncrystalline Solids,* N. B. Hannay, Ed., Plenum, New York, 1976, Chap. 7.
24. J. D. Hoffman, *Polymer,* **24,** 3 (1983).
25. J. D. Hoffman, L. J. Frolen, G. S. Ross, and J. I. Lauritzen, Jr., *J. Res. Natl. Bur. Stand.,* **79A**(6), 671 (1975).

Received June 24, 1992
Accepted August 3, 1992